


AUTHOR QUERY FORM

	Journal: YFGBI Article Number: 2351	Please e-mail or fax your responses and any corrections to: E-mail: corrections.essd@elsevier.sps.co.in Fax: +31 2048 52799
---	--	--

Dear Author,

Please check your proof carefully and mark all corrections at the appropriate place in the proof (e.g., by using on-screen annotation in the PDF file) or compile them in a separate list. To ensure fast publication of your paper please return your corrections within 48 hours.

For correction or revision of any artwork, please consult <http://www.elsevier.com/artworkinstructions>.

Any queries or remarks that have arisen during the processing of your manuscript are listed below and highlighted by flags in the proof. Click on the 'Q' link to go to the location in the proof.

Location in article	Query / Remark: click on the Q link to go Please insert your reply or correction at the corresponding line in the proof
<u>Q1</u>	Please provide the year in references 'Calderon et al. (xxxx) and Sosinska et al. (xxxx)'.
<u>Q2</u>	Please provide the volume number and page range in references 'Klis et al. (2009a)'.
	<p>Answer Q1: (2010) (2011)</p> <p>Answer Q2: 27: 489-93</p> <ul style="list-style-type: none"> - line 33, Abstract: remove "and in the bud scars" - line 238, replace analyzes with analyses - Page 5, Fig. 1E: please align text with spot lines as in the original figure - Page 7, line 455: remove bud scars as indicated. - " , line 479: remove "and" - " , line 482: add E where indicated - " , line 483-484: delete part of the sentence as indicated - Page 10, lines 720-721-722: please delete as indicated - Page 12, line 851: insert space because it is the beginning of a new sentence.

Thank you for your assistance.

18 May 2011

Highlights

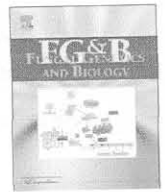
► We examined the localization of a fusion of the *Candida albicans* Phr1 protein with the green fluorescent protein. ► Phr1p-GFP localizes to sites of active cell or hyphal wall formation. ► Phr1p-GFP localization in the hyphal septa requires microtubules polymerization. ► Actin cytoskeleton is required for apical localization of Phr1p-GFP. ► The absence of Phr1p affects hyphal wall organization.



Contents lists available at ScienceDirect

Fungal Genetics and Biology

journal homepage: www.elsevier.com/locate/yfgbi



Phr1p, a glycosylphosphatidylinositol-anchored $\beta(1,3)$ -glucanoyltransferase critical for hyphal wall formation, localizes to the apical growth sites and septa in *Candida albicans*

Enrico Ragni^{a,1}, Julia Calderon^{a,1}, Umberto Fascio^b, Matthias Sipiczki^c, William A. Fonzi^d, Laura Popolo^{a,*}

^aDipartimento di Scienze Biomolecolari e Biotecnologie, Università degli Studi di Milano, 20133 Milano, Italy

^bCentro Interdipartimentale di Microscopia Avanzata (C.I.M.A.), Università degli Studi di Milano, 20133 Milano, Italy

^cDepartment of Genetics and Applied Microbiology, University of Debrecen, H-4010 Debrecen, Hungary

^dDepartment of Microbiology and Immunology, Georgetown University, Washington, DC, USA

ARTICLE INFO

Article history:
Received 9 July 2010
Accepted 3 May 2011
Available online xxxx

Keywords:
Candida albicans
Family GH72
Glucanoyltransferases
Cell wall
Hyphal growth
Morphogenesis

ABSTRACT

Cell wall biogenesis is a dynamic process relying on the coordinated activity of several extracellular enzymes. *PHR1* is a pH-regulated gene of *Candida albicans* encoding a glycosylphosphatidylinositol-anchored $\beta(1,3)$ -glucanoyltransferase of family GH72 which acts as a cell wall remodelling enzyme and is crucial for morphogenesis and virulence. In order to explore the function of Phr1p, we obtained a green fluorescent protein (GFP) fusion to determine its localization. During induction of vegetative growth, Phr1p-GFP was concentrated in the plasma membrane of the growing bud, in the mother-bud neck, in the septum and in the bud scars. Phr1p-GFP was recovered in the detergent-resistant membranes indicating its association with the lipid rafts as the wild type Phr1p. Upon induction of hyphal growth, Phr1p-GFP highly concentrated at the apex of the germ tubes and progressively distributed along the lateral sides of the hyphae. Phr1p-GFP also labelled the hyphal septa, where it colocalized with chitin. Localization to the hyphal septa was perturbed in nocodazole-treated cells, whereas inhibition of actin polymerization hindered the apical localization. Electron microscopy analysis of the hyphal wall ultrastructure of a *PHR1* null mutant showed loss of compactness and irregular organization of the surface layer. These observations indicate that Phr1p plays a crucial role in hyphal wall formation, a highly regulated process on which morphogenesis and virulence rely.

© 2011 Elsevier Inc. All rights reserved.

1. Introduction

Fungal walls are the first interface between the microorganisms and their environment. In fungal pathogens, the cell envelope is greatly involved in virulence since it mediates processes such as adhesion, invasion of the epithelia layers and interaction with the immune cells. In *Candida albicans* the cell wall greatly contributes to its virulence potential. Virulence also relies on the capability of this microorganism to adapt in different niches of the human body. Beside the availability of nutrients and trace elements, dynamic changes in ion concentration, serum concentrations and osmotic pressure, compartments of the human body colonized by *C. albicans* also vary in pH. In particular, pH can be slightly alkaline as in the bloodstream (pH 7.3), close to neutrality, as in organs like

the kidney, liver and duodenum, or acidic, as in the stomach (pH ~2) or vagina (pH ~4.5). Several *C. albicans* genes are regulated by extracellular pH through Rim101-dependent or independent pathways (Bensen et al., 2004; Lotz et al., 2004; Porta et al., 1999; Ramon et al., 1999). Among the genes regulated by Rim101p, albeit in opposite directions, are *PHR1* and *PHR2* (pH-responsive genes 1 and 2) which were also the first identified pH-regulated genes in *C. albicans* (Muhlschlegel and Fonzi, 1997; Saporito-Irwin et al., 1995). *PHR1* is expressed at pH values of 5.5 or higher, whereas *PHR2* is expressed at pH values of 5.5 or lower. *PHR1* and *PHR2* encode glycoproteins highly similar to Gas1p from *Saccharomyces cerevisiae* and Gel1p from the fungal pathogen *Aspergillus fumigatus*. By using *in vitro* assays, Phr/Gas/Gel proteins were shown to cleave internally a $\beta(1,3)$ -glucan chain (the donor) and transfer the non-reducing portion to a new $\beta(1,3)$ -glucan chain (the acceptor) resulting in the elongation of the chain (Mouyna et al., 2000). This activity has great importance in fungal biology for glucan remodelling, which requires a balance between hydrolysis and new incorporation of $\beta(1,3)$ -glucan into the cell wall. Since $\beta(1,3)$ -glucan is a hallmark component of nearly all fungi, fungal

* Corresponding author. Address: Università degli Studi di Milano, Dipartimento di Scienze Biomolecolari e Biotecnologie, Via Celoria 26, 20133 Milano, Italy. Fax: +39 (0) 2 50314895.

E-mail address: Laura.Popolo@unimi.it (L. Popolo).

¹ These authors equally contributed to the work.

species so far sequenced have homologs of the PHR/GAS/GEL families which altogether belong to family GH72 of transglycosidases (Henrissat and Davies, 2000; Ragni et al., 2007b).

The lack of Phr1p or Phr2p dramatically affects *C. albicans* morphogenesis in a manner that is dependent on ambient pH (Fonzi, 1999). Consistent with the expression pattern, $\Delta phr1$ cells exhibit a defective phenotype which is not apparent at pH 5.5 or 6 but becomes visible at pH 7.5 and culminates at pH 8. In the yeast morphology at pH 7.5 or 8, $\Delta phr1$ cells appeared round, multi-budded and larger than the wild type with a swollen aspect similarly to *S. cerevisiae* cells deleted in *GAS1* (Popolo et al., 1993; Saporito-Irwin et al., 1995). In conditions of hyphal growth, $\Delta phr1$ cells produce enlarged and shorter germ tubes (Saporito-Irwin et al., 1995). Additionally, *PHR1* null mutants have a reduction in cell wall $\beta(1,3)$ -glucan content and a more than fivefold increase of chitin accumulation during vegetative growth at the restrictive pH (Fonzi, 1999; Popolo and Vai, 1998). Conversely, deletion of *PHR2* results in a morphogenetic defect which is expressed at acidic pH (Muhlschlegel and Fonzi, 1997). Consistent with the dependence of phenotype on pH, a *PHR1* null mutant was avirulent in a mouse model of systemic infection and as virulent as the wild type in a vaginal infection in rats (De Bernardis et al., 1998). The virulence phenotype of a *PHR2* null mutant was the inverse. The severe morphogenic defects of the *PHR1* null mutant result in an inability to invade epithelia in an *in vitro* reconstituted system and to adhere efficiently to abiotic surfaces and cell monolayers (Calderon et al., xxxx). These traits may contribute to the avirulent phenotype of this mutant.

Beside *PHR1* and *PHR2*, three other paralogs were identified in *C. albicans* genome and named *PHR3*, *PGA4* and *PGA5*. These genes appear to function in conditions which differ from those of *PHR1* and *PHR2* and deletion of either *PHR3* or *PGA4* does not impact growth, dimorphism or virulence (Eckert et al., 2007). Expression of *PGA4* was up-regulated approximately 2-fold during infection but was independent of ambient pH (Eckert et al., 2007). All the products of the *PHR* multigene family are predicted to be anchored to the membrane through a glycosylphosphatidylinositol (GPI). Moreover, Phr1, Phr2 and Pga4 proteins were detected in a proteomic analysis of covalently bound cell wall proteins, also termed the "cell wall proteome" (de Groot et al., 2004; Klis et al., 2009b; Sosinska et al., xxxx). The linkage of many mannoproteins to the cell wall results from further processing of the GPI anchor after reaching the plasma membrane (Van Der Vaart et al., 1996). The distribution between the plasma membrane and the cell wall is affected by the amino acids proximal to the GPI signal and by the long serine and threonine rich regions (Frieman and Cormack, 2003; Frieman and Cormack, 2004). A still unidentified transglycosylase was proposed to catalyze the transfer of a lipid-less portion of the GPI-anchor to the glucan network resulting in cross-linking through a $\beta(1,6)$ -glucan bridge (Klis et al., 2009a). This may promote exposure of the protein at the cell surface. Thus, similar to Gas1p, which is predominantly in the plasma membrane but with a fraction also cross-linked to the cell wall, *C. albicans* Phr1 and

Pga4 proteins could be processed in an analogous manner. In *S. cerevisiae*, a fraction of the cell-wall bound form of Gas1p is specifically localized to the chitin ring and later in the bud scars, where it remains for several generations (Rolli et al., 2009).

In this work we studied the localization of a hybrid between Phr1p and the green fluorescent protein (GFP) during different morphological states in *C. albicans*. Phr1p-GFP localization to multiple sites both in vegetative growth and during hyphal development underlines the crucial role played by this protein in sustaining apical growth in *C. albicans* morphogenesis. The ultrastructure of the hyphal walls revealed striking differences compared to the wild type hyphae indicating the importance of Phr1p for wall assembly during hyphal growth at alkaline pH.

2. Methods

2.1. Strains and growth conditions

The *C. albicans* strains used in this study are listed in Table 1. *C. albicans* cells were routinely grown at 25 °C or 30 °C in YPD (1% yeast extract, 2% Bacto-peptone, 2% glucose) or synthetic minimal medium (SD) (Difco yeast nitrogen base w/o amino acids 6.7 g/liter, 2% glucose). For Ura⁺ strains media, except when used for selection of Ura⁺ transformants, were supplemented with 50 mg of uridine per liter. When media with a defined pH were necessary, 150 mM HEPES [4-(2-Hydroxyethyl) piperazine-1-ethanesulfonic acid sodium salt, Sigma Aldrich] was added to the other components and the pH of the medium was adjusted to the required pH before sterilization. Solid medium was prepared as described above with the addition of 2% bacto-agar. Growth was monitored as the increase in optical density at 600 nm (*OD*₆₀₀). For growth with yeast morphology, cells were grown in YPD or YPD-150 mM HEPES buffered at the required pH at 25 °C. To induce hyphal growth in liquid medium, yeast cells were cultured overnight to stationary phase at 30 °C in YPD or alternatively, when testing Phr1⁻ phenotype, in YPD-150 mM HEPES buffered at pH 6. The stationary-phase cells were inoculated at a density of 2.5×10^6 – 5×10^6 cells/ml in either pre-warmed α -MEM [Alpha MEM w/o ribonucleosides, w/o deoxyribonucleosides, w/o NaHCO₃, (Invitrogen)] or Medium 199 [M199 + Earle's salts + L-Glutamine and w/o aminoacids (Gibco)] at 37 °C. Inducing media were buffered with 150 mM HEPES to pH 7.5 or 8 and glucose concentration was adjusted to 2%. Formation of germ tubes and hyphae was monitored with an Olympus BX60 microscope at different time points following induction (from 30 min to 7 h). Percentage of germ tubes was determined by counting the number of cells with or without germ tubes under the microscope.

2.2. Construction of *PHR1*-GFP expressing strains

For the construction of a chimera of Phr1p with the green fluorescent protein (GFP), internal tagging was required. Tagging immediately after the N-terminal signal peptide was unsuccessful

Table 1
C. albicans strains used in this work.

Strains	Parent	Genotype	Reference
CAF3-1	SC5314	<i>ura3</i> Δ :: <i>imm434</i> / <i>ura3</i> Δ :: <i>imm434</i>	Lab stock
CAS6	CAF3-1	<i>phr1</i> Δ :: <i>hisG</i> / <i>PHR1</i> <i>ura3</i> Δ :: <i>imm434</i> / <i>ura3</i> Δ :: <i>imm434</i>	Saporito-Irwin et al. (1995)
CAS8	CAS6	<i>phr1</i> Δ :: <i>hisG</i> / <i>phr1</i> Δ <i>ura3</i> Δ :: <i>imm434</i> / <i>ura3</i> Δ :: <i>imm434</i>	Saporito-Irwin et al. (1995)
JC-94	CAF3-1	<i>ura3</i> Δ :: <i>imm434</i> / <i>ura3</i> Δ :: <i>imm434</i> <i>PHR1</i> / <i>PHR1</i> -GFP	This work
UBP8	JC-94	<i>URA3</i> / <i>ura3</i> Δ :: <i>imm434</i> <i>PHR1</i> / <i>PHR1</i> -GFP	This work
CAS22	CAS6	<i>phr1</i> Δ :: <i>hisG</i> / <i>PHR1</i> -GFP <i>ura3</i> Δ :: <i>imm434</i> / <i>ura3</i> Δ :: <i>imm434</i>	This work
CAI10	CAF3-1	<i>URA3</i> / <i>ura3</i> Δ :: <i>imm434</i>	Fonzi and Irwin (1993)
CAS10	CAS8	<i>phr1</i> Δ :: <i>hisG</i> / <i>phr1</i> Δ <i>URA3</i> / <i>ura3</i> Δ :: <i>imm434</i>	Calderon et al. (xxxx) and Saporito-Irwin et al. (1995)
CAS-11	CAS-8	<i>phr1</i> Δ :: <i>hisG</i> / <i>PHR1</i> -pUC18- <i>URA3</i> - <i>phr1</i> Δ <i>ura3</i> Δ :: <i>imm434</i> / <i>ura3</i> Δ :: <i>imm434</i>	Saporito-Irwin et al. (1995)

Please cite this article in press as: Ragni, E., et al. Phr1p, a glycosylphosphatidylinositol-anchored $\beta(1,3)$ -glucanoyltransferase critical for hyphal wall formation, localizes to the apical growth sites and septa in *Candida albicans*. Fungal Genet. Biol. (2011), doi:10.1016/j.fgb.2011.05.003

179 so we proceeded with the C-terminal tagging. The sequence encod- 228
 180 ing GFP was inserted between the amino acids G489 and G490. By 229
 181 using a PCR-based strategy, we amplified the GFP-URA3-GFP (GUG) 230
 182 cassette from the GUG plasmid (Gerami-Nejad et al., 2009; Hau- 231
 183 sauer et al., 2005) (kindly gifted by Judith Berman and Cheryl Gale). 232
 184 This strategy is based on the use of 100 bp of homology flanking 233
 185 regions to direct gene targeting (Gola et al., 2003). The cassette car- 234
 186 ried incomplete copies of GFP flanking the counterselectable URA3 235
 187 marker and was amplified with the pair of long primers GPFOR2 236
 188 and GPREV2 shown in Table 2 (Biomers, Germany). The 5' portions 237
 189 (100nt for both GPFOR2 and GPREV2) were complementary to the 238
 190 *PHR1* sequence flanking the site selected for the insertion and the 239
 191 3' segments (in italics) were complementary to the *GFP* sequences 240
 192 present in the GUG plasmid. For simplicity we named the amplified 241
 193 cassette GUG-PHR1-100. The ~3.37 kb PCR product was used to 242
 194 transform strain CAF3-1 using the LiAcetate procedure (Walther 243
 195 and Wendland, 2003a). Ura⁺ transformants were checked by PCR 244
 196 for correct integration of the cassette into *PHR1* using several diag- 245
 197 nostic primers. Then, cells were plated onto SD plates containing 246
 198 625 µg/ml of 5-FOA to promote the excision of the *URA3* marker 247
 199 which restores a functional GFP gene in frame with the coding se- 248
 200 quences of *PHR1*. Proper excision of *URA3* was assessed by different 249
 201 diagnostic primers. For this purpose genomic DNA was extracted 250
 202 from different clones. The sequence of all diagnostic primers used 251
 203 is available upon request. Two out of 35 clones were positive and 252
 204 were further tested for phenotype. Three different clones (JC-93, 253
 205 JC-94 and JC-95) exhibited a similar phenotype and bright green 254
 206 fluorescence. They were converted to Ura3⁺ by integration of the 255
 207 genomic fragment containing *URA3* and *IRO1* derived from the 256
 208 digestion of pLUBP with *Bgl*III and *Pst*I. Cells were transformed with 257
 209 the gel-purified *Bgl*III/*Pst*I genomic fragment of about 5 Kbp and 258
 210 Ura⁺ clones were selected. Genomic DNA from control strains 259
 211 and from Ura⁺ clones was extracted and subjected to different 260
 212 diagnostic PCR reactions using two pairs of primers: URA3For2/UR- 261
 213 A3Rev and URA3For/URA3Rev2 (Table 2). Three different clones (8, 262
 214 10 and 16) were further examined and tested for filamentation. 263
 215 They were phenotypically identical and clone 8, renamed strain 264
 216 UBP8, was used as a representative one in this work. 265

217 To test the functionality of *PHR1-GFP* we constructed a strain, 266
 218 where only *Phr1p-GFP* was expressed. CAS-6 strain was trans- 267
 219 formed with a GUG cassette flanked by 200-bp of *PHR1* sequences 268
 220 flanking the tagging site. The extension of the cassette ends of fur- 269
 221 ther 100 bp was obtained in two steps. First, the GUG-PHR1-100 270
 222 cassette was amplified with the oligos GPFOR2 and GPREV2 using 271
 223 pGUG as template. The ~3.37 kb product was cloned in the pCRII- 272
 224 TOPO vector (Invitrogen) to generate the GUG-100 plasmid. The 273
 225 cloned fragment was sequenced to check for absence of errors 274
 226 (BMR Genomics, Padova). Then, 20 ng of pGUG-100 were used in 275
 227 50-µl reactions with Phusion DNA polymerase (NEB) and GPFOR3

and GPREV3 oligonucleotides (Table 2). These primers carry at 228
 the 5'-end additional 100 nt of *PHR1* segments flanking the se- 229
 lected tagging site and at their 3' end 20 nt overlapping the ends 230
 of the GUG-100 cassette. About 30 µg of the ~3.57 Kbp amplified 231
 product, named GUG-PHR1-200, were used to transform CAS-6 232
 (*PHR1/phr1Δ*) cells. Two independent clones (10 and 22) harboured 233
 the correct integration and were plated on 5-FOA plates as de- 234
 scribed above. The lack of errors in the integrated sequence was 235
 checked by sequencing PCR products from genomic DNA. Several 236
 Ura⁺ colonies derived from clone 22 were characterized and exhib- 237
 ited a bright fluorescence. More detailed analyzes concentrated on 238
 four clones that were positive to the PCR tests on genomic DNA for 239
 excision of the *URA3* marker. A representative clone (CAS22) is de- 240
 scribed in detail shown in this work. 241

2.3. Microscopy

242
 243 Cells were routinely observed by phase-contrast microscopy and 244
 scored for budding or germ tube formation by counting at least 245
 200 cells after mild sonication. For green fluorescence microscopy 246
 cells were either analyzed without fixation or with fixation. In both 247
 cases, cells were mildly sonicated by two cycles of 6 s, before being 248
 processed. For observation without fixation, cells were collected by 249
 centrifugation at 6000 g for 2 min, washed twice with PBS, pH 7.4 250
 at 4 °C and incubated at least 15 min on ice before being examined 251
 under the microscope. If DNA nuclear staining was necessary, it 252
 was performed on formaldehyde-fixed cells by using 5 µg/ml of 253
 4,6-diamidino-2-phenylindole (DAPI) and viewed under UV. As de- 254
 scribed previously (Warenda and Konopka, 2002), fixation did not 255
 exceed 15 min in cells, where visualization of GFP was necessary. 256
 Staining of chitin was performed using Calcofluor white (Sigma, 257
 St. Louis, Mo.). Calcofluor was added to the culture at a concentra- 258
 tion of 0.2 µg/ml during the last 10 min of growth before viewing 259
 the cells as it has been described previously (Warenda and 260
 Konopka, 2002).

261 The cells were examined as wet mounts using an Olympus BX60 262
 or Leica DM RX2 fluorescence microscopes. For confocal 263
 microscopy cells were examined using a Leica TCS SP2 AOBs (Leica 264
 Microsystems, Heidelberg, Germany) confocal laser-scanning 265
 microscope, equipped with an Ar/Kr and He/Ne lasers and a PLAPO 266
 63 oil immersion objective. *Phr1p-GFP* as excited with a laser line 267
 of 488 nm and the fluorescence was collected between 493 and 268
 539 nm. DAPI or Calcofluor were excited in the UV ($\lambda = 364$ nm) 269
 and the fluorescence was collected in the range 410 and 470 nm. 270
 A series of horizontal focal section was collected by sequential 271
 scanning of samples with a 1 µm step size.

272 For actin staining, about 2×10^7 cells were fixed in 3.7% formal- 273
 274 dehyde for 2 h at room temperature. Then, the suspension was 275
 centrifuged and the pellet was washed twice with 1 ml of distilled 276

Table 2
Oligonucleotides used in this work.

Name	Sequence 5'-3'
GPFOR2	TGATTTCAAAGGCAGTGCCTTCAATCAATATCAAGCCTAGTCTAGTGGCAGCTGCAAAGCTGTTACTGGAGTAGCTACTGTAAGGCATCT TCCTCTGGTGGTGGTCTTAAAGGTGAAGAATTATCACTCGG (underlined: nucleotides encoding two glycine residues that function as linker amino acids; in italics: sequence complementary to <i>GFP</i> in pGUG)
GPREV2	GAGTTGCTTTAACTCCAGAGCTTGAGCTGGACCCAGAGCTGCTGCTGCTTGATGATCCAGAAGTAGATGCAGAGGAAGATCCAGATTGGAG CTTCTTTGTACAATTCATCCATAC (in italics: sequence complementary to <i>GFP</i> in pGUG)
GPFOR3	AAGGGAATAATGGTGTGCTTCTCTCTGCTGATAAAGATCGTTTGCAATATGTTGAAACCAGATTACCTTGACCAAGACAAGAAATCCACTGCT TGTGATTTCAAAGGCAGTGCCTT (underlined: sequence complementary to <i>PHR1</i> in pGUG-100)
GPREV3	ATCGGTTAGTCTTCATGATTAAAAACAACGGACATACCAACAATGACAGTAACAATAGTAATAATTGAAACCAATTTGACCATAGACATTT GTTGAGTTGCTTTAACTCCAGAG (underlined: sequence complementary to <i>PHR1</i> in pGUG-100)
URA3For2	GCATGCTGTCCTGGGAA
URA3Rev	TACTACTAGTGGTGGCGG
URA3For	CTGTTGTGACATCAACTG
URA3Rev2	TTCCACGTGACACCATGAGC

275 water (dH₂O). Cells were resuspended in 500 µl of PBS. After a mild
276 sonication, 20 µl of Rhodamine-phalloidin solution (Molecular
277 Probes) was added and samples were incubated for 45 min in the
278 dark. After two washes with 1 ml of PBS, cells were observed under
279 the microscope.

280 For Electron Microscopy, cells were harvested from a 100 ml
281 culture by centrifugation at 3000g for 10 min and washed twice
282 in dH₂O. The pellet was resuspended in 5 ml of freshly-made
283 potassium permanganate (2% in dH₂O) and incubated at 4 °C for
284 60 min. Fixed cells were collected by centrifugation, washed three
285 times in dH₂O and embedded in agar blocks, dehydrated in ethanol
286 of increasing concentrations and infiltrated with araldite mixture.
287 Thin sections were cut from the hardened araldite blocks by dia-
288 mond knives. To enhance contrast, the sections were stained with
289 Reynolds solution for 10 min and with 25% uranyl acetate for
290 20 min at room temperature. Specimens were examined in a Jeol
291 1010 electron microscope and photos were taken with Veleta Soft
292 Imaging System.

293 **2.4. Extract preparation, electrophoresis and immunoblotting**

294 About 2 × 10⁸ cells were collected by filtration, washed and
295 resuspended in ice-cold dH₂O. After a 2-min centrifugation at
296 4 °C the pellets were quickly frozen and stored at -20 °C. After
297 thawing, 500 µl of SB-minus buffer (0.0625 M Tris-HCl pH 6.8,
298 5% SDS) supplemented with protease inhibitors [1 mM phenyl-
299 methylsulfonyl fluoride, 1 µg/ml pepstatin and Protease Inhibitor
300 Cocktail Complete (Roche) prepared as a 25× stock in dH₂O] was
301 added to each pellet. After addition of an equal volume of cold glass
302 beads, cells were broken by shaking in a FastPrep 120 for 45 s alter-
303 nating with 1-min incubations on ice. Unbroken cells and glass
304 beads were removed by a 5-min centrifugation at 11,500g at
305 4 °C. Protein concentration was determined by the DC Protein As-
306 say (Bio-Rad). SDS-PAGE and immunoblotting were performed as
307 described previously using large slab gels (Gatti et al., 1994; Ragni
308 et al., 2007a). Monoclonal mouse anti-actin monoclonal antibody
309 (mAb) clone C4 (MP Biomedicals) was used at a dilution of
310 1:1000 in TBS-BSA, 0.1% Tween20. Mouse anti-GFP mAb (Roche)
311 was used at a dilution of 1:4000 in TBS-BSA, 0.1% Tween 20. Perox-
312 idase-conjugated affinity purified F(ab')₂ fragment donkey anti-
313 rabbit or anti-mouse IgG were from Jackson Laboratories and used
314 at a dilution of 1:10000. Bound antibodies were revealed using the
315 ECL Western blotting detection reagents (Amersham Pharmacia
316 Biotech). Densitometric measurements of under-saturated films
317 were performed using the program Scion Image.

318 **2.5. DRMs isolation**

319 Isolation of detergent resistant membranes (DRMs) was per-
320 formed essentially as previously described (Bagnat et al., 2000).
321 *C. albicans* cells (50 OD₆₀₀) were collected from a culture in expo-
322 nential growth phase in YPD-pH 8. Cells were mechanically broken
323 at 4 °C in a FastPrep 120 in 1 ml of TNE buffer (50 mM Tris-HCl, pH
324 7.4, 150 mM NaCl and 5 mM EDTA) supplemented with protease
325 inhibitors and glass beads as described above. The lysate was
326 cleared by centrifugation at 500g for 5 min at 4 °C. The cleared ly-
327 sate (~900 µl) was incubated in 1% Triton X-100 and TNE buffer
328 plus protease inhibitors for 30 min at 4 °C in a final volume of
329 1.5 ml. The treated lysate (between 2.5 and 4 mg) was adjusted
330 to 40% OptiPrep (Sigma-Aldrich) and the resulting mixture
331 (4.2 ml) was sequentially overlaid with 6.7 ml of 30% OptiPrep in
332 TNEX buffer (TNE buffer including 0.1% Triton X-100) supple-
333 mented with protease inhibitors and 1.1 ml of TNEX buffer. The
334 samples were centrifuged at 100,000g in an SW41Ti rotor for
335 2.5 h. At the end 0.9-ml fractions were collected from the top of

the gradient. Proteins were precipitated with 10% TCA on ice and
analyzed by Western blot.

338 **3. Results**

339 **3.1. Construction of a GFP tagged version of Phr1p**

340 In order to study the localization of Phr1p we constructed a
341 GFP-tagged version. Phr1p contains both a secretory signal se-
342 quence at the N-terminus and a GPI-attachment signal at the C-ter-
343 minus, and therefore GFP was inserted internally. For this purpose,
344 we used a *GFP-URA3-GFP* construct that directed a PCR-mediated
345 two step insertion of GFP internal to the coding sequences of
346 *PHR1* (Gerami-Nejad et al., 2009; Hausauer et al., 2005). We also
347 exploited the identification of successful tagging sites in the *S. cere-*
348 *visiae* Gas1p, which shares 55% amino acid identity with Phr1p
349 (Rolli et al., 2009). The first selected site was between residues
350 S24 and S25, just after the predicted signal peptide. This construct
351 gave unsatisfactory results since the fluorescence was very weak.
352 As an alternative, GFP was placed inside the C-terminal region be-
353 tween G489 and G490 located before the predicted GPI attachment
354 site at residue S517 (De Groot et al., 2003). As depicted in the
355 scheme of Fig. 1A, this insertion site was just at the beginning of
356 the Serine-rich region and was chosen on the basis of three criteria
357 (i) the Ser-rich region functions as a disordered spacer and is dis-
358 pensable for *in vitro* activity and *in vivo* functionality of Gas1p
359 (Gatti et al., 1994; Popolo et al., 2008), (ii) the insertion site is
360 downstream of the two functional domains, GH72 and Cys-box/
361 X8, which were shown to be essential for Gas1p functionality
362 and are conserved also in Phr1p (Popolo et al., 2008) and (iii) the
363 analogous insertion site in Gas1p gave origin to a partially func-
364 tional fluorescent protein (Rolli et al., 2009). A representative clone
365 harbouring one allele of *PHR1* and the fusion *PHR1-GFP* at the place
366 of the second allele is here described (Table 1).

367 As expected, the fusion gene maintained the same expression
368 profile as *PHR1*. In conditions that promote growth in yeast mor-
369 phology, Phr1p-GFP was detected in cells at alkaline pH but not at
370 acidic pH (Fig. 1B). The apparent MW of the polypeptide was about
371 115 kDa, as expected for a protein constituted by Phr1p (88 kDa)
372 and GFP (~30 kDa). The Phr1p-GFP was also produced upon induc-
373 tion of hyphal growth. The immunoblot of Fig. 1C shows that the fu-
374 sion protein was absent at time zero but was already detectable at
375 30 min after the induction and its level increased during the process
376 of hyphae formation. Cell morphology, growth rate at alkaline pH,
377 kinetics of filamentation of this strain were identical to those of
378 the parental strain (data not shown). Microscopic analysis showed
379 that Phr1p-GFP hybrid protein was fluorescent in living cells (see
380 below).

381 To assess the functionality of Phr1-GFP we replaced the *PHR1*
382 allele of the heterozygous strain *CAS6 (phr1Δ/PHR1)* with the
383 *PHR1-GFP* fusion. Different clones carrying *PHR1-GFP* were ana-
384 lyzed and a representative one (*CAS22*) is described hereafter.
385 Phr1p-GFP alone suppressed the growth defect of the *PHR1* null
386 mutant during growth in yeast form in media buffered at pH 8, a
387 very restrictive condition for the mutant (Saporito-Irwin et al.,
388 1995). The growth rates were 0.27 ± 0.01 (*n* = 3) for the Phr1⁻ cells
389 (*CAS8*), 0.34 ± 0.02 (*n* = 4) for cells carrying only Phr1p-GFP
390 (*CAS22*) and 0.36 ± 0.01 (*n* = 3) for the parental strain (*CAF3-1*)
391 Moreover, Phr1p-GFP complemented the swollen, large and multi-
392 budded aspect typical of Phr1⁻ cells (Fig. 1D). Thus, Phr1p-GFP fully
393 complemented the defects of the *PHR1* null mutant during growth
394 in yeast form. Concerning the cell wall defects of *Δphr1* cells, we
395 tested the sensitivity to calcofluor (CF), a cell wall perturbing agent
396 that binds and interfere with the assembly in microfibrils of nas-
397 cent chitin chains. Phr1⁻ cells are known to have an increased chi-

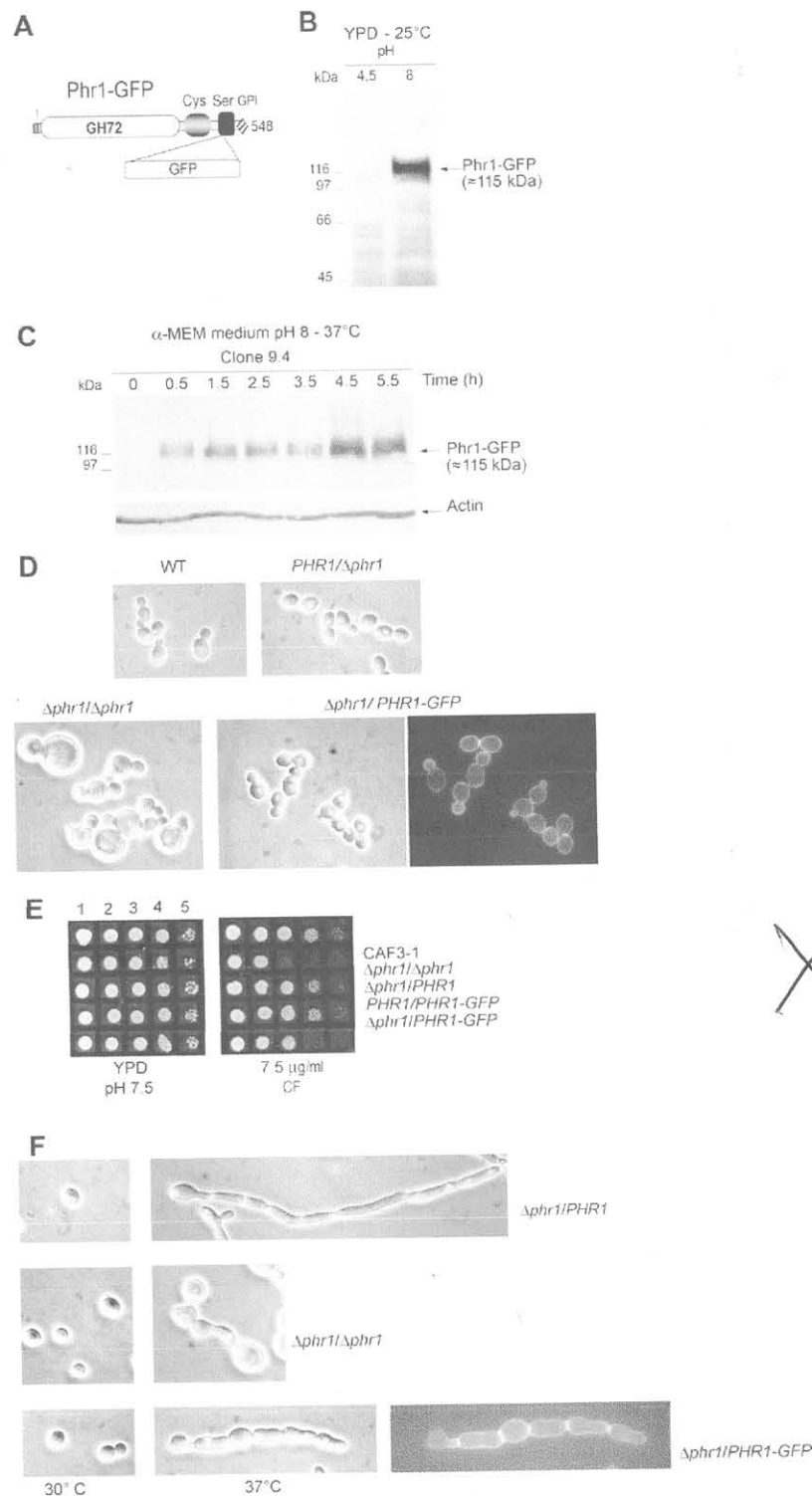


Fig. 1. Expression and functionality of the Phr1p-GFP hybrid protein. (A) Schematic representation of the insertion site of GFP in the amino acid sequence of Phr1p. GH72: signature domain of family 72 of transglycosidases; Cys: cysteine-enriched module (also named X8); Ser: serine-rich domain and GPI: signal for GPI attachment. In the grey box is the signal peptide (aa 1–21). (B) Total protein extracts (~200 µg), from strain JC-94 (*PHR1/PHR1::GFP*) exponentially growing in the indicated conditions were analyzed by immunoblot with an anti-GFP mAb. (C) Total extracts from JC-94 under hyphal growth inducing conditions. The upper part of the filter was immunodecorated with an anti-GFP mAb, whereas the lower part with an anti-actin mAb. (D) Full complementation of the morphogenic defects of Phr1⁻ cells by one copy of *PHR1::GFP* during growth in yeast form in YPD-150 mM HEPES buffered at pH 8 at 25 °C. Phase-contrast and GFP fluorescence microscopy analyzes are shown. (E) Test of CF sensitivity of the indicated strains. 3 µl of a concentrated suspension (5 × 10⁸ cells/ml) of exponentially growing cells (1) and of 10× (2), 100× (3), 1000× (4) and 10,000× (5) dilutions were spotted on YPD pH 7.5 plates in the absence or presence of calcofluor (CF) and incubated for 2 days at 30 °C. (F) Test of functionality of Phr1-GFP during hyphal growth. Hyphae formation was induced by shifting stationary phase cells pre-grown in YPD buffered at pH 6 at 30 °C to M199 buffered at pH 8 at 37 °C and incubated overnight. Microscopy analysis of the indicated strains is shown.

398 tin content that is required for the compensation of cell wall defects
399 and be hypersensitive to this drug (Fonzi, 1999; Popolo and
400 Vai, 1998). Whereas one copy of *PHR1* was able to fully suppress
401 the CF sensitivity of $\Delta phr1$ cells, one copy of *PHR1-GFP* conferred
402 a 10-fold increase in resistance but not a full suppression indicat-
403 ing a partial complementation of the defect (Fig. 1E).
404 To complete the analysis, we monitored hyphae formation.
405 *PHR1* null mutant is unable to support hyphal growth and at alkaline
406 pH it forms short enlarged germ tubes with wider septa (Cald-
407 eron et al., xxxx; Saporito-Irwin et al., 1995). As shown in Fig. 1F
408 (upper panel), one copy of *PHR1* was sufficient to suppress the defects
409 in hyphal growth of $\Delta phr1$ cells. One copy of *PHR1-GFP* did
410 not affect early germ tube formation but elongation was affected.
411 Hyphae were septate but the single compartments appeared swollen.
412 These results suggest that the hybrid protein suppresses the defect
413 in the septum but is not sufficient to confer resistance to the lateral
414 hyphal wall which enlarges and gives rise to pseudo-hyphae-like
415 structures. The fluorescence signal of GFP was intense in the septa,
416 where the protein concentrates and weaker in the lateral walls (Fig. 1F
417 lower panel). Overall, these results indicate that in the absence of stress
418 in the yeast form, Phr1-GFP alone fully complements the morphogenic
419 defects of the *PHR1* null mutant indicating that it is functional. However,
420 Phr1-GFP alone is not sufficient to counteract a severe challenge to cell
421 wall integrity

as imposed by CF or hyphal wall formation. For this reason the rest
of the work was performed using cells carrying the wild type allele
together with the *PHR1-GFP* fusion.

3.2. *Phr1p-GFP* localizes to the plasma membrane, bud neck and septum

The localization of Phr1p-GFP was analyzed during growth in yeast form. Taking advantage of the conditional nature of the *PHR1* expression, we monitored the localization of Phr1p-GFP upon a shift of stationary phase cells to a condition that induces the expression of the hybrid protein (pH 7.5) and promotes growth in the yeast morphology (25 °C). Cells were stained with Calcofluor (CF) to simultaneously examine Phr1p-GFP (green fluorescence) and chitin (blue fluorescence). In stationary phase cells no fluorescence was detected (data not shown). After one doubling of the OD₆₀₀ of the culture, Phr1p-GFP nicely decorated the cell periphery in accordance with the predicted localization to the plasma membrane (Fig. 2A). In small buds, a bright signal was distributed all over the plasma membrane indicating a concentration of the protein in the area of active cell wall expansion (Fig. 2A, thin arrow). In addition, in medium-budded cells two bright green fluorescent dots were detected at both sides of the mother-daughter neck (Fig. 2A, inset). The presence of bright patches that overlapped

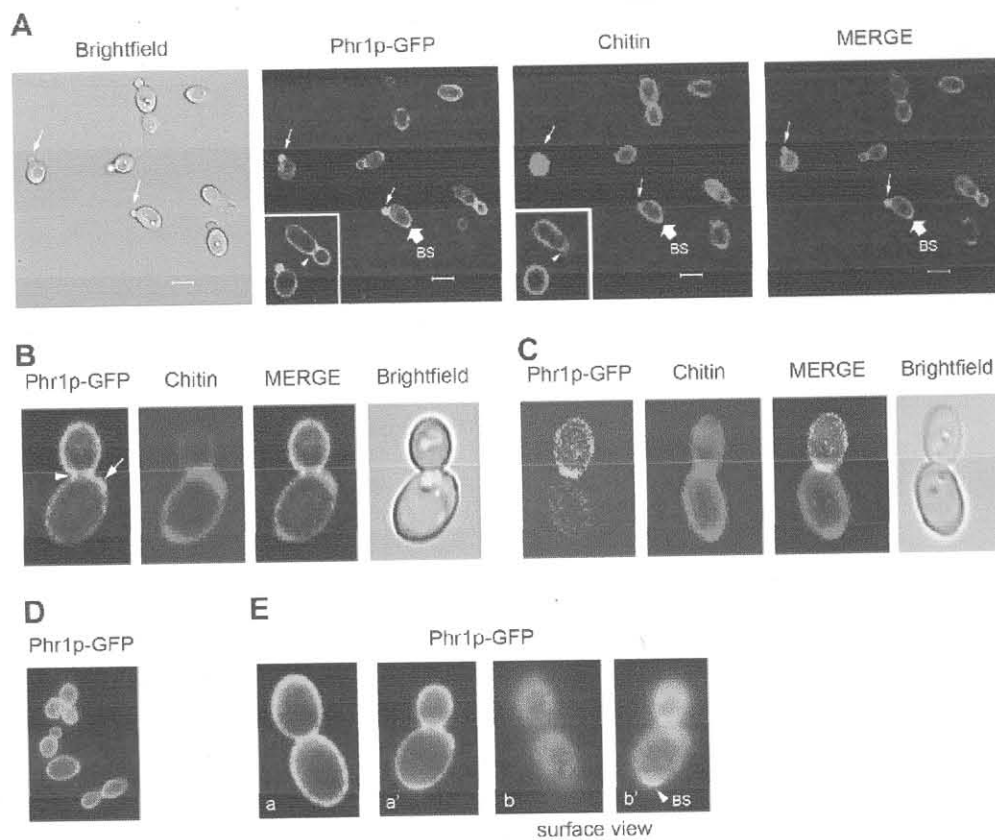


Fig. 2. Localization of *Phr1p-GFP* and chitin in *C. albicans*. (A) Cells (strain JC-94) were grown to stationary phase in YPD at 25 °C, then collected and transferred to YPD-150 mM HEPES, pH 7.5 at 25 °C (initial OD₆₀₀ ~ 0.35) to induce the expression of *Phr1p-GFP*. After one doubling (OD₆₀₀ ~ 0.7), the localization of *Phr1p-GFP* (green fluorescence) and chitin (blue fluorescence) were examined. Confocal micrographs show the presence of *Phr1p-GFP* at the plasma membrane, with a higher intensity around the small bud (thin arrow). The protein concentrates in the bud neck (arrowhead) and at the bud scars (thick arrow). In the merged image, the overlap of the green and blue fluorescence creates a light blue color. The growing bud is green indicating the absence of chitin. In the inset: a median optical section plane shows in more detail the localization at the bud neck (arrowhead) and around the growing bud. BS: bud scar. Bar: 5 μM. (B) Detail of *Phr1p-GFP* and chitin localizations in a medium-budded cell. The arrowhead indicates the presence of *Phr1p-GFP* at the bud neck. The thin arrow indicates the lateral view of a bud scar adjacent to the neck, where blue and green signal overlap and produce a light blue (merge). (C) Detail of the septum region of a large-budded cell. *Phr1p-GFP* concentrates at the septum, delineating a thick line overlapping with chitin. (D) In log-phase *Phr1p-GFP* is distributed over the mother and daughter plasma membrane. (E) Detail of cells showing the fluorescence at the periphery (a and a') and discontinuous (a) and a surface view (b and b') of the same cells showing a pattern of fine dots and a bud scar (arrowhead). The cells in the images b and b' are deliberately out-of-focus. BS: Bud scar.

Please cite this article in press as: Ragni, E., et al. *Phr1p*, a glycosylphosphatidylinositol-anchored β(1,3)-glucanoyltransferase critical for hyphal wall formation, localizes to the apical growth sites and septa in *Candida albicans*. Fungal Genet. Biol. (2011), doi:10.1016/j.fgb.2011.05.003

with chitin, suggested a further localization of Phr1p-GFP to the bud scars (Fig. 2A, thick arrow). The pattern of CF labelling (blue fluorescence) indicated the presence of chitin at the cell periphery, at the bud neck (chitin ring) and the septum but chitin was absent in small buds. This is in agreement with previous studies that showed the lack of chitin deposition in the growing bud in *S. cerevisiae* (Cabib and Duran, 2005). Yet in the large bud, chitin was present, consistent with deposition of chitin occurring in the daughter cell wall after cytokinesis. In the merged image, where the overlapping of the green and blue fluorescence gives rise to a light blue, Phr1p-GFP appeared to co-localize with chitin to the periphery of unbudded cells, mother cells and large buds, to the bud neck, septum and bud scar (Fig. 2A). Small to medium-size buds showed exclusively the presence of Phr1p-GFP. Fig. 2B shows in more detail the Phr1p-GFP localization to both sides of the bud neck overlapping with the chitin ring that encircles the bud neck (arrowhead). The fluorescence at the bud neck forms a ring as also observed by the analysis of different optical sections (data not shown). Moreover, it can be seen the localization of Phr1p-GFP to a bud scar that is adjacent to the bud neck (Fig. 2B, arrow). In addition, Fig. 2C shows Phr1p-GFP forming a thick line over the entire septum region in a large-budded cell. In order to determine whether Phr1p was also localized to the inner plane of the septum, sections of a confocal microscopy analysis were examined. Phr1p-GFP was present along the septum line also in the median optical sections (data not shown). This suggests that at the end of cytokinesis, Phr1p-GFP also localizes to the primary septum or in close proximity to it (either secondary septa or plasma membrane sides facing the secondary septa).

After one more doubling, the culture was in balanced exponential growth-phase. In these cells, Phr1p-GFP fluorescence was observed not only in the daughter cells, but was distributed over the surface of mother cells, indicating an association with both polarized growth of the bud and isotropic growth of the mother cell (Fig. 2D). Upon closer examination, the fluorescence appeared discontinuous along the cell contour in many cells (Fig. 2E, a). In addition, when the focus was moved at the cell surface a pattern of fine dots was visible suggesting a possible association with plasma membrane microdomains (Fig. 2E, b and b'). Also rings of bright fluorescence were detected, corroborating the localization of Phr1p-GFP to the bud scars (Fig. 2B and b' arrowhead).

In conclusion, Phr1p-GFP has four localization sites: the cell periphery, the chitin ring, the bud scar and the primary septum or a site close to it. Therefore, the protein appears to concentrate preferentially in the region of cell wall formation, as the growing bud and septum. In the latter localization the protein co-localizes with chitin. A similar localization was previously shown for Gas1p-GFP (Rolli et al. 2009) although in *C. albicans* it has been more difficult to detect Phr1p-GFP in the bud scars probably due the concomitant presence of the wild type protein which may dilute the intensity of the fluorescent signal. Similarly to Gas1p, Phr1p-GFP seems to concentrate in plasma membrane microdomains.

3.3. Phr1p-GFP segregates in microdomains of the plasma membrane

In a previous proteomic study Phr1p was detected among the proteins present in lipid rafts (Insenser et al., 2006). To assess whether the GFP-tagged Phr1p was enriched in lipid rafts we purified them and assayed for the presence of GFP-tagged Phr1p. Due to their particular lipid composition, namely abundance of sterols and sphingolipids, lipid rafts are resistant to solubilization with detergents at 4 °C. Because of this property, they are often referred to as "detergent resistant membranes" or DRMs. The low buoyant density of lipid rafts was exploited to isolate them by centrifugation on density gradients. To determine whether Phr1p-GFP was

sequestered in lipid rafts, extracts were prepared and processed by a floatation assay on density gradients. Gradient fractions were analyzed by immunoblot using an anti-GFP mAb or polyclonal anti-ScGas1p antibodies which recognize Phr1p (Popolo and Vai, 1998; Vai et al., 1996). As shown in Fig. 3A, in the parental strain Phr1p was detected as an 88 kDa-polypeptide in fraction 2 at the top of the gradient. This fraction is enriched in plasma membrane lipid rafts since it contains Pma1p, the plasma membrane H⁺-ATPase (Insenser et al., 2006; Martin and Konopka, 2004). Phr1p-GFP was detected as a 115 kDa-polypeptide and was recovered in the same position at the top of the gradient (Fig. 3B). Both Phr1p and Phr1p-GFP and their immature forms of higher electrophoretic mobility were detected in other fractions (9 to bottom), where the membrane compartments of the secretory pathway as well as cytoplasmic fractions separate and, where the majority of the protein is recovered (Aronova et al., 2007 and our unpublished data). It seems that a greater proportion of the Phr1p-GFP was present in these fractions suggesting a slower maturation/transport of the Phr1-GFP precursors. Overall these results indicate that the presence of Phr1p-GFP in the plasma membrane microdomains reflect the segregation of a small fraction of the protein in the raft domains of the plasma membrane, whereas a great fraction is distributed in other fractions.

In order to compare the level of Phr1p-GFP with respect to wild type Phr1p expressed in the same strain, an immunoblot from cells expressing Phr1-GFP was reacted with anti-ScGas1p antibodies (Fig. 3C). The lipid rafts fraction at the top of the gradient (fraction 2) showed the 115 kDa-polypeptide of Phr1-GFP, a cross-reactive band of about 113 kDa and the 88 kDa-band corresponding to Phr1p. The ratio between the intensities of the Phr1p-GFP and the Phr1p was about 0.25. The fact that the level of Phr1p-GFP is lower than the level of the protein expressed from the wild type allele, suggests that Phr1p-GFP is either less efficiently transported along the secretory pathway and/or subjected to a higher turnover in the plasma membrane with respect to Phr1p.

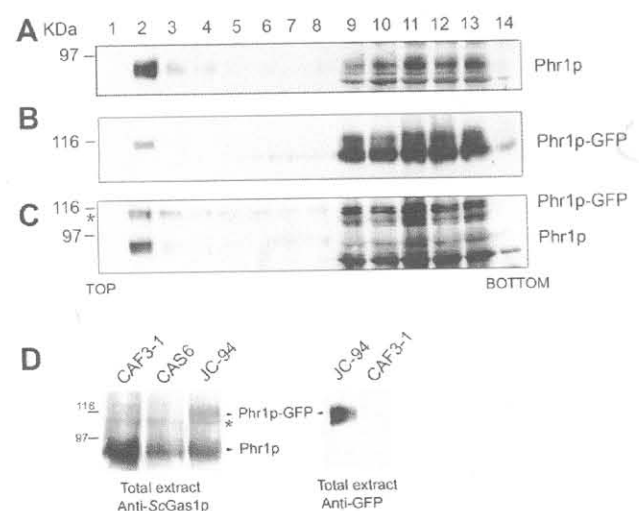


Fig. 3. Phr1p and Phr1p-GFP associates with the detergent-resistant membranes. Cells extracts were treated as described under Materials and Methods. Fractions (1–14) of the Optiprep density gradients were collected from the top. (A) Immunoblot with anti-ScGas1p serum (cross-reacting with Phr1p) of fractions from CAF3-1. (B) Immunoblot of fractions from JC-94 (PHR1/PHR1-GFP) obtained with anti-GFP mAb. (C) Immunoblot of fractions from JC-94 obtained using anti-ScGas1p polyclonal antibodies. The band in fraction 2 indicates the presence of Phr1p-GFP (115 kDa) or Phr1p (88 kDa) in the lipid rafts. (D) Immunoblot of the total protein extracts (about 200 µg) from cells with two copies of PHR1 (CAF3-1), one copy of PHR1 (CAS6) and one copy of PHR and one copy of PHR1-GFP (JC-94). The asterisk labels a cross-reactive band.

543 We also compared the levels of the hybrid and wild type proteins in total extracts. A densitometric analysis of blots from two
544 independent experiments was performed. A representative one is shown in Fig. 3D. In total extracts only the mature proteins were
545 detectable. As expected, Phr1p expressed from one allele of *PHR1* was ~50% the amount of Phr1 protein expressed from the parental
546 strain carrying two alleles. In *PHR1/PHR1-GFP* cells, the wild type Phr1p was still expressed at roughly the same level as in the hetero-
547 zygous strain, whereas the level of Phr1-GFP (115 kDa) was about half of it. Thus, in lipid rafts only half of the total mature fusion
548 protein is recovered.

554 **3.4. Phr1p-GFP localization during hyphal growth**

555 In order to analyze the localization of Phr1p-GFP during hyphal growth, cells were induced to form hyphae. As shown in Fig. 4, at
556 time zero no green fluorescence was detected in agreement with the lack of *PHR1* expression in stationary phase cells. At 30 min,
557 Phr1p-GFP was clearly visible at the tip of the germ tubes, sometimes forming a neat crescent. At 1 h, the fluorescence was highly
558 concentrated at the tip of the germ tubes but it was also visible in the subapical region, whereas the blastospore was totally nega-
559 tive. At 3 h, Phr1p-GFP signal was very bright at the hypha apex but it was also distributed along the lateral sides of the hyphae. Inter-
560 estingly, Phr1p-GFP was also visible in the first septum of the germ tubes. At 5.5 h, Phr1p-GFP was still concentrated at the hypha apex
561 but it also labelled uniformly the lateral sides of the hyphae and also nicely labelled the hyphal septa (Fig. 4, arrows). In conclusion,
562 Phr1p-GFP is highly polarized at the apex of the hypha, where the activity of extension of the cell wall is more intense but it also dis-
563 tributes along the lateral sides of the hypha as it extends. The latter location suggests that Phr1p might be required for continuous
564 remodelling of lateral hyphal walls. In addition, Phr1p localized to the septa which are also sites of wall formation.

575 **3.5. Phr1p-GFP colocalizes with chitin in the septa and lateral cell walls of the hyphae but not at the apex**

577 To investigate the localization of Phr1p-GFP in the septa, cells undergoing hyphal growth were stained with CF. At 1 h from
578 induction of hypha formation, cells showed the typical localization of Phr1p-GFP with a strong labelling at the apical and subapical
579 part of the hypha, along the lateral walls and in the first septum
580
581

but no fluorescence was seen in the blastospore. On the contrary, chitin was more abundant in the blastospore, at the base of the
582 germ tube and in the septum but relatively less abundant at the apex. In the merge image, chitin and Phr1p-GFP appeared to colo-
583 calize at the septum and in the lateral walls but not at the apex portion, where the Phr1p-GFP signal appeared very strong and chitin
584 was relatively weak (Fig. 5A). At 3 h (Fig. 5B), the hyphae were more elongated and Phr1p-GFP was still at the apical and subapical
585 regions but it was also distributed gradually along the lateral cell walls. Moreover, Phr1p-GFP was highly concentrated in the hyphal
586 septa. Chitin was more abundant along the lateral cell walls and in the septa but less at the apical part of the hypha. Thus, Phr1p-GFP
587 co-localized with chitin in the lateral cell walls and in the septa but not at the apical region (Fig. 5B, merge). These results strongly sup-
588 port the notion that Phr1p-GFP localizes to regions, where the wall is more plastic to allow extension. In agreement with this, chitin is
589 less abundant in these regions since the cross-linking of wall components with chitin is presumed to confer resistance to the walls.
590 The analysis of the optical sections indicated that Phr1p-GFP was also seen in the inner part of the septum forming a single line (data
591 not shown).

603 **3.6. Role of the cytoskeleton in the localization of Phr1p-GFP during hyphal growth**

605 The presence of Phr1p-GFP in different sites of the growing hypha, prompted us to examine whether the microtubules or the actin
606 cytoskeleton were contributing to these localizations. Cells were treated with nocodazole (NZ) whose efficacy as microtu-
607 bule-depolymerizing agent in *C. albicans* was previously established (Rida et al., 2006; Yokoyama et al., 1990) or cytochalasin A
608 (CA) to inhibit actin polymerization (Crampin et al., 2005; Rida et al., 2006).

609 Cells were pre-grown in YPD and diluted to OD = 0.2 in hyphal growth inducing conditions in the absence or presence of different
610 concentrations of NZ (from 1.5 to 20 µg/ml), added at time zero. The efficacy of NZ was assayed by monitoring the inhibition of nu-
611 clear divisions and the optimal concentration of NZ was 20 µg/ml in agreement with a previous report (Yokoyama et al., 1990). At
612 this concentration, the inhibitor did not affect the ability of the germinating cells to form germ tubes but caused a marked reduction
613 of mitosis. After 1.5 h of treatment, the percentage of cells with divided nuclei was 35% (n = 217) in the control cells and only 6.7%
614
615
616
617
618
619
620
621
622

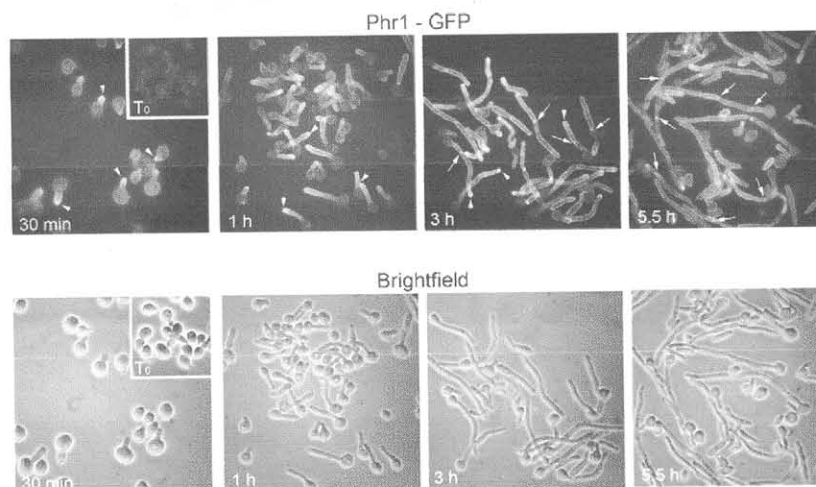


Fig. 4. Localization of Phr1p-GFP during hyphal growth. Micrographs show strain UBP8 at time zero and at the indicated times after a shift of stationary phase cells to medium M199-150 mM HEPES pH 7.5 at 37 °C. The green fluorescence of Phr1p-GFP is absent at time zero (inset). The arrowhead indicates the high concentration of protein at the tip of the germ tubes or at the apical portion of the hyphae. The thin arrow indicates the presence of Phr1p-GFP at the septa.

Please cite this article in press as: Ragni, E., et al. Phr1p, a glycosylphosphatidylinositol-anchored β(1,3)-glucanoyltransferase critical for hyphal wall formation, localizes to the apical growth sites and septa in *Candida albicans*. Fungal Genet. Biol. (2011), doi:10.1016/j.fgb.2011.05.003

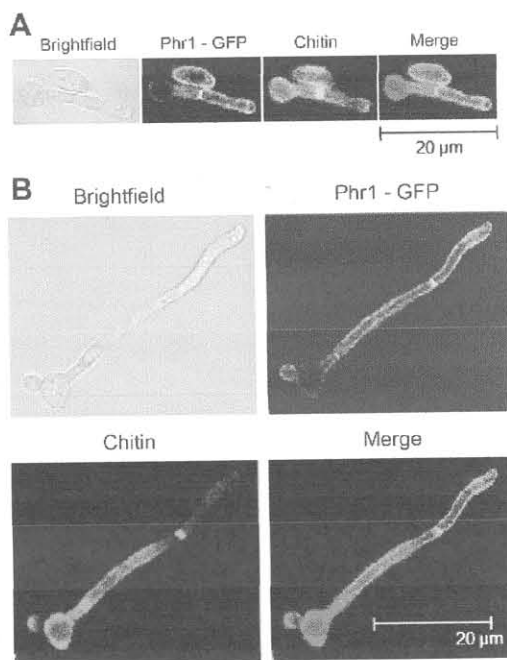


Fig. 5. *Phr1p*-GFP and chitin colocalize at the septa and in lateral walls but not in the apex of the hypha or in the blastospore. (A) Confocal micrographs of JC-94 cells at 1 h after the induction of hyphal growth. *Phr1p*-GFP (green) and chitin (blue). (B) Confocal micrographs of JC-94 cells at 3 h after the induction. The merge of the green and blue fluorescence gives origin to a light blue fluorescence. (For interpretation of the references to colour in this figure legend, the reader is referred to the web version of this article.)

($n = 221$) in the NZ-treated culture. As shown in Fig. 6A the nucleus remained in the blastospore of treated cells in agreement with the lack of nuclear migration, a microtubule-driven event (Finley and Berman, 2005). Next, we examined *Phr1p*-GFP localization. At 30 min after germ tube induction, *Phr1p*-GFP localized to the tip of the germ tube both in treated and untreated cultures (Fig. 6B). After 1.5 h, *Phr1p*-GFP localized to the apical and subapical regions and also in lateral walls of the hyphae (Fig. 6C). Interestingly, *Phr1p*-GFP localization to the septal sites was severely affected. The green fluorescence was more intense and diffused at the presumptive septum site, as ascertained by chitin staining with CF. These results reveal that inhibition of microtubule polymerization interferes with septum formation and causes abnormal chitin deposition which may perturb the regular localization of *Phr1p*-GFP at the septal sites. In conclusion, the inhibition of microtubule polymerization by NZ does not affect polarization of *Phr1p*-GFP at the tip of the germ tubes or at the apex of the hyphae but has a strong effect on the localization to the hyphal septa. These results also demonstrate that microtubules play a role in the proper formation of the hyphal septa in *C. albicans*. In order to rule out that this effect was due to a synergism between CF and NZ we examined the effect of NZ in a culture where CF was not added. In this case also, *Phr1p*-GFP localization to the septa was perturbed (data not shown).

To investigate the effects of inhibition of the actin cytoskeleton we induced hyphal growth in the presence or absence of 20 μg/ml of CA added at time zero. As shown in Fig. 7A, CA abolished actin cytoskeleton polarization and prevented germ tube formation as reported by others (Rida et al., 2006; Yokoyama et al., 1990). At 45 min after drug addition, *Phr1p*-GFP was visualized in punctuate intracellular structures and cells were mostly weakly fluorescent or negative, indicating that the transport of *Phr1p*-GFP is actin-dependent and the protein is retained in intracellular vesicular

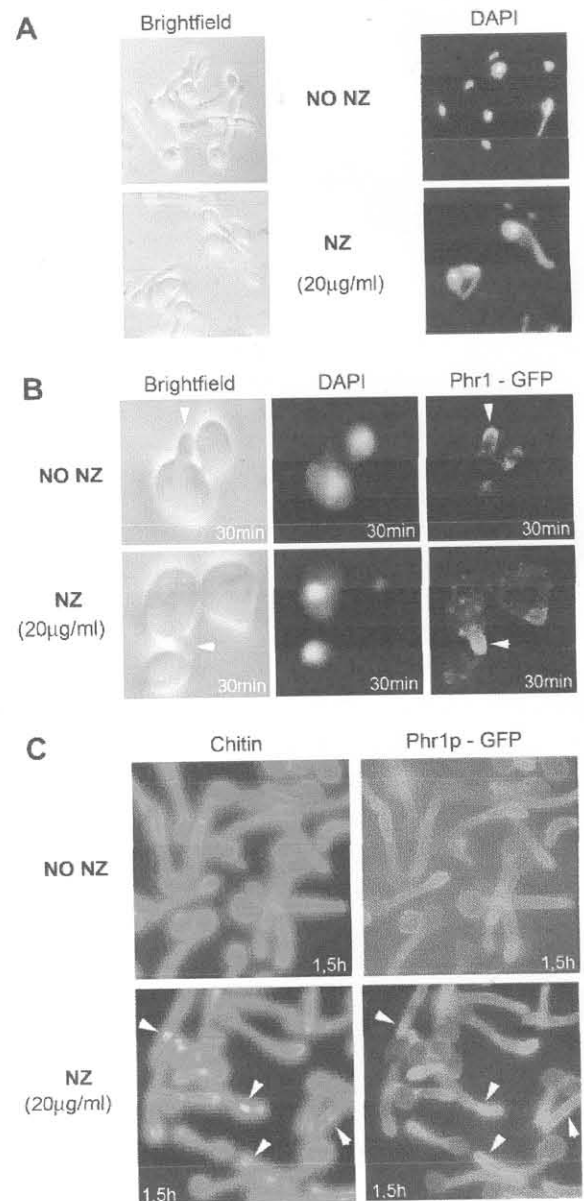


Fig. 6. Effect of nocodazole (NZ) on *Phr1p*-GFP localization during hyphal growth. Cells (strain UBPS) were induced to form hyphae in medium M199–150 mM HEPES pH 7.5 at 37 °C in the absence or presence of NZ. (A) NZ, added at time zero, inhibits nuclear divisions during germ tube elongation (1.5 h). (B) Confocal micrographs of emerging germ tubes at 30 min after induction (C) NZ affects septa formation and *Phr1p*-GFP localization at the septa or at the presumptive septum sites. Arrowhead indicates abnormal chitin deposition and altered *Phr1p*-GFP localization at the presumptive septa. Chitin staining was performed by adding CF to the culture 10 min before collecting the cells.

compartments if actin is not polarized. At 70 min after CA addition, no green fluorescence was detectable suggesting that the protein was degraded and *PHR1* expression switched off due to inhibition of growth (data not shown).

Finally, we also tested the effect of CA added 2 h after the induction of hyphal growth. After 30 min of treatment, actin cytoskeleton was depolarized (Fig. 7C). Interestingly, after 30 min of treatment *Phr1p*-GFP fluorescence was very weak both at the apex and in lateral sides of the hyphae compared to the untreated cells (Fig. 7D). In addition, dot-like structures were detected in the cytoplasm of some hyphae in agreement with a block of vesicle trans-

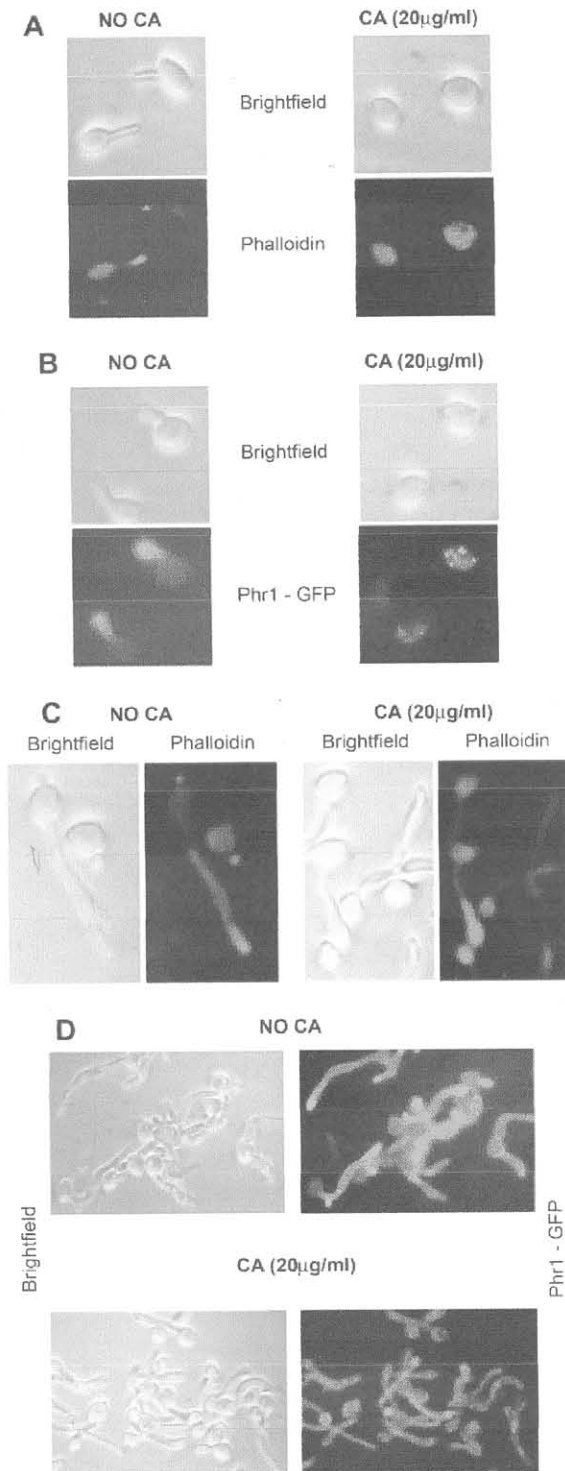


Fig. 7. Effect of Cytochalasin A (CA) on Phr1p-GFP localization. Cells were induced to form hyphae in M199–150 mM HEPES, pH 7.5 at 37 °C. (A) CA was added at time zero and 45 min later Phalloidin staining was performed. (B) Inhibition of actin polymerization abolished Phr1p-GFP transport to the cell surface concomitantly with the inhibition of germ tube formation. (C) CA was added 2.5 h after induction of hyphal growth and cells were analyzed 30 min later. Phalloidin staining indicates the efficacy of the drug. (D) The green fluorescence was weak and diffuse in the cytoplasm with an occasional punctuate pattern. (For interpretation of the references to colour in this figure legend, the reader is referred to the web version of this article.)

In conclusion, the cytoskeleton plays different roles in Phr1p-GFP localization. The polarization of the protein to the apex is actin-dependent in agreement with the essential role of actin cytoskeleton in hyphal polarized growth and localization of cell-surface material (Anderson and Soll, 1986; Novick and Botstein, 1985; Sudbery et al., 2004). Interestingly, localization of Phr1p-GFP along the lateral sides of the hypha also required the actin cytoskeleton suggesting that not only secretion but also endocytosis, two processes depending on actin, might be involved in the localization of Phr1p in lateral sides of the hyphae. The Phr1p-GFP localization at the septa depends on microtubule polymerization that is required for septum formation.

3.7. Lack of Phr1p causes an abnormal hyphal wall structure

To explore more deeply the role of Phr1p in the hyphal wall biogenesis, we analyzed the effect of the lack of Phr1p on hyphal cell wall ultrastructure. A *PHR1* null mutant and its parental strain were pre-grown in YPD–150 mM HEPES, pH 6. At this pH, $\Delta phr1$ mutant phenotype is not yet manifested but the expression of *PHR1* was reduced to a minimum and thus also its potential interference in assessing the effects of *PHR1* deletion. Stationary phase cells were inoculated into M199–150 mM HEPES, pH 7.5 at 37 °C to induce hyphal growth. At 2 h following induction, cells were processed for Electron Microscopy analysis (EM). As shown in Fig. 8A, in the control strain (CAI-10) the cell wall and hyphal wall were continuous and their structure was similarly organized. An electron-dense outermost layer was detected and beneath it an electro-transparent layer. These layers correspond to the external layer of mannoproteins and to the glucan layer respectively. This was seen also in more detail in Fig. 8B and C. Interestingly, in some mutant cells it was possible to distinguish the cell wall of the blastospore and the germ tube at the site of their connection. At this site, the regular organization of the cell wall disappeared and a very irregular structure appeared in the emerged tube (Fig. 8D). The most striking differences of the mutant wall were the crenate aspect of the mannoprotein layer and lack of a uniform thickness (Fig. 8D–E). Since there is a lag in the appearance of the phenotype, the altered wall was present in some cells at the apical portion of abnormal hyphae (Fig. 8E and G). In some hyphae the apex was swollen and this probably caused a distension of the wall as shown in Fig. 8H.

In conclusion, lack of Phr1p has a dramatic effect on hyphal wall ultrastructure. The EM micrographs suggest a lack of coherence between the layers and an imbalance in the assembly of the inner glucan network perhaps resulting in a loose connection of the mannoproteins to the underneath glucan network which gives rise to the wavy aspect of the hyphal wall surface.

4. Discussion

In this work we investigated the localization of a fluorescent version of Phr1p during growth of *C. albicans* in the yeast form and in the yeast-to-hypha transition. In the yeast morphological state, Phr1p showed three localization sites: (i) in the plasma membrane (ii) in the chitin ring and (iii) in the bud scars. In the plasma membrane, Phr1p-GFP was concentrated in very fine surface dots potentially representing plasma membrane microdomains. Phr1p and Phr1p-GFP conformed to the operative criteria used to assess whether a protein is sequestered in lipid rafts. This result is also in agreement with a previous report (Insenser et al., 2006), where Phr1p was identified by proteomic techniques in lipid rafts and with the presence of the homologous ScGas1p in rafts domains of budding yeast (Aronova et al., 2007;

port. The arrest of hyphal growth hampered the evaluation of the effects on septum formation.

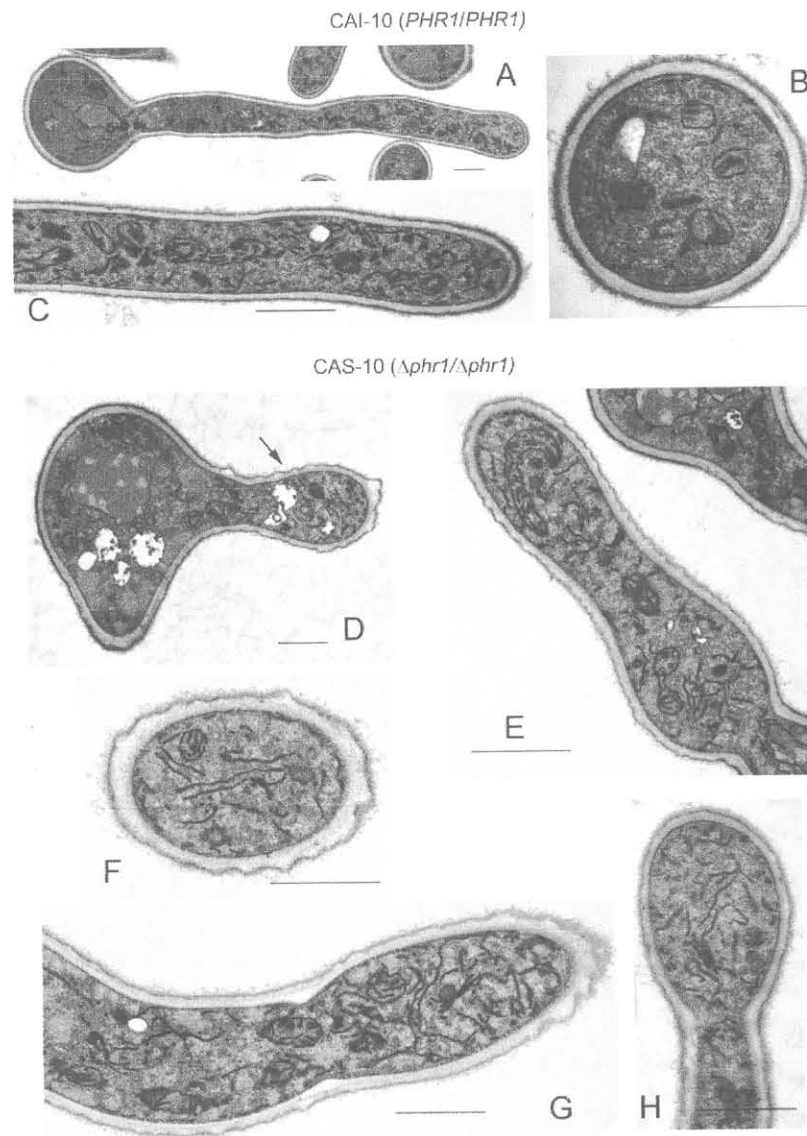


Fig. 8. Cell wall ultrastructure of the *PHR1* null mutant during hyphal growth. Wild type cells and *PHR1* null mutant were induced to form hyphae in M199–150 mM HEPES, pH 7.5 at 37 °C. (A) Wild type hypha shows a regular wall structure. (B) A cross section. (C) Detail. (D) Emerging germ tube and evagination. The arrow indicates the crenate surface of the germ tube wall. (E) Abnormal apical and subapical portion of a hypha. (F) Cross-section. (G) Apical region with a “weavy” aspect. (H) Detail of a swollen apex. Bar: 1 μ m.

730 Rolli et al., 2009). Lipid rafts are important organizing centres for
731 protein sorting, signalling and cell polarity (Alvarez et al., 2007).
732 In general, GPI-anchored proteins preferentially cluster in lipid
733 rafts which may also fuse to form larger domains named SRDs (sterol-
734 rich domains) (Alvarez et al., 2007).
735 In experiments of induction of exponential growth phase
736 Phr1p-GFP was preferentially localized to the plasma membrane
737 of the bud. Labelling was not confined to the bud tip, as occurs
738 for proteins involved in the establishment of polarity, but rather
739 it was distributed over the entire periphery suggesting that Phr1p
740 function is required for bud wall expansion. Interestingly, this
741 localization reflects the distribution of cortical actin in the growing
742 bud of *C. albicans* (Anderson and Soll, 1986). In log-phase cells the
743 protein was localized over the entire periphery of both mother and
744 daughter cells indicating that at steady state the protein is probably
745 required also for glucan remodelling of the mother cell wall
746 during isotropic growth. Overall the localizations of Phr1p in *C.*

albicans resembles that of Gas1p-GFP in *S. cerevisiae* (Rolli et al.,
2009).

In *S. cerevisiae*, we demonstrated a further localization of Gas1p-GFP in, or close to, the primary septum in cells that had undergone cytokinesis (Rolli et al., 2009). By examining optical sections perpendicular to the plane of the septum we observed that Phr1p also localized to the site of primary septum in large budded cells (Fig. S1B). Thus, Phr1p may also be localized to the primary septum or in close proximity to it, such as in the secondary septa or in the daughter and mother plasma membranes when the cells are close to cell division. The primary septum is a chitinous disk that is synthesized by the essential enzyme Chs1p in *C. albicans* and by Chs2p in *S. cerevisiae* (Cabib, 2004; Munro et al., 2001). In both microorganisms the primary septum is encircled by the chitin ring in vegetatively growing cells. The fact that the localizations of Phr1p and Gas1p are similar is consistent with the capability of ectopically expressed *PHR1* to fully replace *GAS1* deletion in *S. cerevisiae* cells (Vai et al., 1996).

Please cite this article in press as: Ragni, E., et al. Phr1p, a glycosylphosphatidylinositol-anchored $\beta(1,3)$ -glucanoyltransferase critical for hyphal wall formation, localizes to the apical growth sites and septa in *Candida albicans*. Fungal Genet. Biol. (2011), doi:10.1016/j.fgb.2011.05.003

747
748
749
750
751
752
753
754
755
756
757
758
759
760
761
762
763

764 Hyphal growth is another distinct morphogenic state in *C. albicans* (Sudbery et al., 2004). Upon induction of hyphal growth, Phr1p-GFP was detectable in as early as 30 min both on western blots and as a fluorescent signal in live cells. The fluorescence was highly polarized to the apex of the germ tube in agreement with a role of Phr1p in the incorporation of the $\beta(1,3)$ -glucan in the area of maximal wall extension. This localization is consistent with the typical growing pattern of a *C. albicans* hypha (Berman, 2006). In hypha, the apical cell has an active cell cycle and is the elongating portion of the hypha, whereas distal cell compartments are arrested in G₁ (Berman, 2006). Interestingly, in *C. albicans* hyphae localization of the Golgi apparatus is restricted to the growing tip of the apical cell (Rida et al., 2006). Phr1 protein, in contrast, is also distributed along the lateral aspect of hypha cells. Lateral localization may occur directly or occur by redistribution from the apex, an issue that will require further investigation. Remodeling of $\beta(1,3)$ -glucans in the lateral wall of hyphae may be required for maintenance of cell shape or continual wall repair. Beside these localizations, Phr1p-GFP also decorated hyphal septa, another important site of wall formation (Walther and Wendland, 2003b). Interestingly, in these sites a minor fraction of actin and also SRDs concentrate (Anderson and Soll, 1986; Martin and Konopka, 2004; Yokoyama et al., 1990).

787 Consistent with the need of a more plastic wall, chitin was relatively less abundant in the apex portion of the hyphae. In contrast, in the lateral walls of the hypha and in the septa, Phr1p and chitin colocalized. In the lateral walls, the cross-links among the wall components are increased and Phr1p could be involved in dynamic processes of the hypha elongation contributing to the plasticity and extension of the apex and additionally to the resistance of the lateral hyphal walls.

795 The localization pattern of Phr1p is entirely consistent with the previously reported morphological phenotypes of a *PHR1* null mutant (Saporito-Irwin et al., 1995). Lack of Phr1p in yeast forms of *C. albicans*, causes an enlargement of the buds and the presence of multi-budded cells indicating a role of Phr1p in determining the proper development of the bud and in facilitating cell division as previously observed for Gas1p (Rolli et al., 2009). The localization observed during hyphal growth defines the importance of Phr1p in hyphal development. Consistent with the requirement for a highly polarized localization of Phr1p at the apex of the growing germ tube, germ tubes produced by the *PHR1* null mutant are short, enlarged and also curved (Saporito-Irwin et al., 1995). At the restrictive pH, $\Delta phr1$ cells are able to induce germ tubes but are defective in supporting their elongation indicating a role of Phr1p localization in the maintenance of hyphal development.

810 Dramatic defects in hyphal wall ultrastructure are described in this work. The hyphal walls exhibited the typical layer structure but the texture appeared loose and the surface had an atypical wavy appearance. Since Phr1p acts as a glucan elongating enzyme, it is conceivable that its absence may increase the amount of short glucan chains and/or limit interconnections within the glucan layer. The attendant loss in structural integrity could cause a loss of resistance and be responsible of the enlargement of the germ tubes (Saporito-Irwin et al., 1995). These data underline the importance of a proper balance between the synthesis and assembly of the hyphal wall components. It is conceivable that the effects on wall structure together with the abnormal morphogenesis, may explain the reported defects of the *PHR1* null mutant in adhesion both to abiotic surfaces and cell monolayers and in invasion of reconstituted human epithelia (Calderon et al., xxxx).

825 In this work we have also studied the role of cytoskeleton in the localization of Phr1p during hyphal growth. The results indicate that microtubules are not required for hyphae formation in agreement with two previous reports (Rida et al., 2006; Yokoyama et al., 1990) or for polarization of Phr1p to the tip of the germ tubes.

However, NZ did perturb septum formation and the localization of Phr1p to the septa. These results indicate that the localization of Phr1p in the septum is tightly coupled with proper septum formation. This effect may be mediated by defects in septin ring formation since septin ring formation at the presumptive septum site is coupled to the events of the nuclear division cycle (Finley and Berman, 2005). Inhibition of actin polymerization prevented germ tube formation in agreement with the well assessed role of actin cytoskeleton in polarized growth in *C. albicans*. Consequently, Phr1p was localized in small dots inside the cells, the majority of which were only weakly fluorescent. In CA-treated hyphae, Phr1p disappeared from the periphery and small dots were detected inside the hyphae. A degradation or repression of *PHR1* expression may occur in the presence of the block of growth and vesicle movement toward the cell surface.

Acknowledgments

The authors thank Roberto Cavatorta for the preparation of the figures, Judith Berman and Cheryl Gale for the GUG plasmid, Neta Dean for the encouragement in this project and Genny Degani for technical assistance. This work was supported by EU-RTN project "Cantrain" N.512481 and PRIN 2007 (Programma di Rilevante Interesse Nazionale) to L.P.S. was a recipient of a Marie Curie contract from "Cantrain". E.R. was a recipient of a Type A contract from Università degli Studi di Milano.

References

- Alvarez, F.J. et al., 2007. Sterol-rich plasma membrane domains in fungi. *Eukaryot. Cell* 6, 755–763.
- Anderson, J.M., Soll, D.R., 1986. Differences in actin localization during bud and hypha formation in the yeast *Candida albicans*. *J. Gen. Microbiol.* 132, 2035–2047.
- Aronova, S. et al., 2007. Probing the membrane environment of the TOR kinases reveals functional interactions between TORC1, actin, and membrane trafficking in *Saccharomyces cerevisiae*. *Mol. Biol. Cell* 18, 2779–2794.
- Bagnat, M. et al., 2000. Lipid rafts function in biosynthetic delivery of proteins to the cell surface in yeast. *Proc. Natl. Acad. Sci. USA* 97, 3254–3259.
- Bensen, E.S. et al., 2004. Transcriptional profiling in *Candida albicans* reveals new adaptive responses to extracellular pH and functions for Rim101p. *Mol. Microbiol.* 54, 1335–1351.
- Berman, J., 2006. Morphogenesis and cell cycle progression in *Candida albicans*. *Curr. Opin. Microbiol.* 9, 595–601.
- Cabib, E., 2004. The septation apparatus, a chitin-requiring machine in budding yeast. *Arch. Biochem. Biophys.* 426, 201–207.
- Cabib, E., Duran, A., 2005. Synthase III-dependent chitin is bound to different acceptors depending on location on the cell wall of budding yeast. *J. Biol. Chem.* 280, 9170–9179.
- Calderon, J. et al., xxxx. *PHR1*, a pH-regulated gene of *Candida albicans* encoding a glucan-remodelling enzyme, is required for adhesion and invasion. *Q1 Microbiology.* 156, 2484–2494.
- Crampin, H. et al., 2005. *Candida albicans* hyphae have a Spitzenkörper that is distinct from the polarisome found in yeast and pseudohyphae. *J. Cell Sci.* 118, 2935–2947.
- De Bernardis, F. et al., 1998. The pH of the host niche controls gene expression in and virulence of *Candida albicans*. *Infect. Immun.* 66, 3317–3325.
- de Groot, P.W. et al., 2004. Proteomic analysis of *Candida albicans* cell walls reveals covalently bound carbohydrate-active enzymes and adhesins. *Eukaryot. Cell* 3, 955–965.
- De Groot, P.W. et al., 2003. Genome-wide identification of fungal GPI proteins. *Yeast* 20, 781–796.
- Eckert, S.E. et al., 2007. PGA4, a GAS homologue from *Candida albicans*, is up-regulated early in infection processes. *Fungal. Genet. Biol.* 44, 368–377.
- Finley, K.R., Berman, J., 2005. Microtubules in *Candida albicans* hyphae drive nuclear dynamics and connect cell cycle progression to morphogenesis. *Eukaryot. Cell* 4, 1697–1711.
- Fonzi, W.A., 1999. *PHR1* and *PHR2* of *Candida albicans* encode putative glycosidases required for proper cross-linking of beta-1, 3- and beta-1, 6-glucans. *J. Bacteriol.* 181, 7070–7079.
- Fonzi, W.A., Irwin, M.Y., 1993. Isogenic strain construction and gene mapping in *Candida albicans*. *Genetics* 134, 717–728.
- Frieman, M.B., Cormack, B.P., 2003. The omega-site sequence of glycosylphosphatidylinositol-anchored proteins in *Saccharomyces cerevisiae* can determine distribution between the membrane and the cell wall. *Mol. Microbiol.* 50, 883–896.

Please cite this article in press as: Ragni, E., et al. Phr1p, a glycosylphosphatidylinositol-anchored $\beta(1,3)$ -glucanoyltransferase critical for hyphal wall formation, localizes to the apical growth sites and septa in *Candida albicans*. *Fungal Genet. Biol.* (2011), doi:10.1016/j.fgb.2011.05.003

- 902 Frieman, M.B., Cormack, B.P., 2004. Multiple sequence signals determine the
903 distribution of glycosylphosphatidylinositol proteins between the plasma
904 membrane and cell wall in *Saccharomyces cerevisiae*. *Microbiology* 150,
905 3105–3114.
- 906 Gatti, E. et al., 1994. O-linked oligosaccharides in yeast glycosyl
907 phosphatidylinositol-anchored protein gp115 are clustered in a serine-
908 rich region not essential for its function. *J. Biol. Chem.* 269, 19695–
909 19700.
- 910 Gerami-Nejad, M. et al., 2009. Additional cassettes for epitope and fluorescent
911 fusion proteins in *Candida albicans*. *Yeast* 26, 399–406.
- 912 Gola, S. et al., 2003. New modules for PCR-based gene targeting in *Candida albicans*:
913 rapid and efficient gene targeting using 100 bp of flanking homology region.
914 *Yeast* 20, 1339–1347.
- 915 Hausauer, D.L. et al., 2005. Hyphal guidance and invasive growth in *Candida albicans*
916 require the Ras-like GTPase Rsr1p and its GTPase-activating protein Bud2p.
917 *Eukaryot. Cell* 4, 1273–1286.
- 918 Henrissat, B., Davies, G.J., 2000. Glycoside hydrolases and glycosyltransferases.
919 Families, modules, and implications for genomics. *Plant. Physiol.* 124, 1515–
920 1519.
- 921 Insenser, M. et al., 2006. Proteomic analysis of detergent-resistant membranes from
922 *Candida albicans*. *Proteomics* 6 (Suppl 1), S74–S81.
- 923 Q2 Klis, F.M. et al., 2009a. Covalently linked wall proteins in ascomycetous fungi. *Yeast*.
924 Klis, F.M. et al., 2009b. Covalently linked cell wall proteins of *Candida albicans*
925 and their role in fitness and virulence. *FEMS Yeast Res.* 9, 1013–
926 1028.
- 927 Lotz, H. et al., 2004. RBR1, a novel pH-regulated cell wall gene of *Candida albicans*, is
928 repressed by RIM101 and activated by NRG1. *Eukaryot. Cell* 3, 776–
929 784.
- 930 Martin, S.W., Konopka, J.B., 2004. Lipid raft polarization contributes to hyphal
931 growth in *Candida albicans*. *Eukaryot. Cell* 3, 675–684.
- 932 Mouyna, I. et al., 2000. Glycosylphosphatidylinositol-anchored glucanosyltrans-
933 ferases play an active role in the biosynthesis of the fungal cell wall. *J. Biol.*
934 *Chem.* 275, 14882–14889.
- 935 Muhlschlegel, F.A., Fonzi, W.A., 1997. PHR2 of *Candida albicans* encodes a functional
936 homolog of the pH-regulated gene PHR1 with an inverted pattern of pH-
937 dependent expression. *Mol. Cell Biol.* 17, 5960–5967.
- 938 Munro, C.A. et al., 2001. Chs1 of *Candida albicans* is an essential chitin synthase
939 required for synthesis of the septum and for cell integrity. *Mol. Microbiol.* 39,
940 1414–1426.
- 941 Novick, P., Botstein, D., 1985. Phenotypic analysis of temperature-sensitive yeast
942 actin mutants. *Cell* 40, 405–416.
- 943 Popolo, L. et al., 2008. Disulfide bond structure and domain organization of yeast
944 beta(1,3)-glucanosyltransferases involved in cell wall biogenesis. *J. Biol. Chem.*
945 283, 18553–18565.
- Popolo, L., Vai, M., 1998. Defects in assembly of the extracellular matrix are
responsible for altered morphogenesis of a *Candida albicans* phr1 mutant. *J.*
Bacteriol. 180, 163–166.
- Popolo, L. et al., 1993. Physiological analysis of mutants indicates involvement of
the *Saccharomyces cerevisiae* GPI-anchored protein gp115 in morphogenesis
and cell separation. *J. Bacteriol.* 175, 1879–1885.
- Porta, A. et al., 1999. PRR1, a homolog of *Aspergillus nidulans* palf, controls pH-
dependent gene expression and filamentation in *Candida albicans*. *J. Bacteriol.*
181, 7516–7523.
- Ragni, E. et al., 2007a. GAS2 and GAS4, a pair of developmentally regulated genes
required for spore wall assembly in *Saccharomyces cerevisiae*. *Eukaryot. Cell* 6,
302–316.
- Ragni, E. et al., 2007b. The Gas family of proteins of *Saccharomyces cerevisiae*:
characterization and evolutionary analysis. *Yeast* 24, 297–308.
- Ramon, A.M. et al., 1999. Effect of environmental pH on morphological development
of *Candida albicans* is mediated via the PacC-related transcription factor
encoded by PRR2. *J. Bacteriol.* 181, 7524–7530.
- Rida, P.C. et al., 2006. Yeast-to-hyphal transition triggers formin-dependent Golgi
localization to the growing tip in *Candida albicans*. *Mol. Biol. Cell* 17, 4364–
4378.
- Rolli, E. et al., 2009. Immobilization of the glycosylphosphatidylinositol-anchored
Gas1 protein into the chitin ring and septum is required for proper
morphogenesis in yeast. *Mol. Biol. Cell* 20, 4856–4870.
- Saporito-Irwin, S.M. et al., 1995. PHR1, a pH-regulated gene of *Candida albicans*, is
required for morphogenesis. *Mol. Cell Biol.* 15, 601–613.
- Sosinska, G.J., et al., xxxx. Mass spectrometric quantification of the adaptations in
the wall proteome of *Candida albicans* in response to ambient pH. *Microbiology.*
157, 136–146.
- Sudbery, P. et al., 2004. The distinct morphogenic states of *Candida albicans*. *Trends.*
Microbiol. 12, 317–324.
- Vai, M. et al., 1996. *Candida albicans* homologue of GGP1/GAS1 gene is functional in
Saccharomyces cerevisiae and contains the determinants for
glycosylphosphatidylinositol attachment. *Yeast* 12, 361–368.
- Van Der Vaart, J.M. et al., 1996. The beta-1,6-glucan containing side-chain of cell
wall proteins of *Saccharomyces cerevisiae* is bound to the glycan core of the GPI
moiety. *FEMS Microbiol. Lett.* 145, 401–407.
- Walther, A., Wendland, J., 2003a. An improved transformation protocol for the
human fungal pathogen *Candida albicans*. *Curr. Genet.* 42, 339–343.
- Walther, A., Wendland, J., 2003b. Septation and cytokinesis in fungi. *Fungal. Genet.*
Biol. 40, 187–196.
- Warena, A.J., Konopka, J.B., 2002. Septin function in *Candida albicans*
morphogenesis. *Mol. Biol. Cell* 13, 2732–2746.
- Yokoyama, K. et al., 1990. The role of microfilaments and microtubules in apical
growth and dimorphism of *Candida albicans*. *J. Gen. Microbiol.* 136, 1067–1075.